Laser Surface Texturing of Metals Using Dynamic Melt Expulsion by Application of Fast Modulated CW-Laser Radiation

Andreas Schkutow* and Thomas Frick

Institute for Chemistry, Materials and Product Development, Technische Hochschule Nürnberg Georg Simon Ohm, Kesslerplatz 12, 90489 Nürnberg, Germany
Corresponding author's e-mail: andreas.schkutow@th-nuernberg.de

Laser surface texturing of metals is usually performed using pulsed laser sources. Short and ultrashort pulsed laser systems offer the highest machining quality and processing flexibility. Most of these beam sources however feature relatively low average powers or high system prices. Continuous wave fiber lasers in comparison feature high average powers at moderate costs. In this work the laser power of a continuous-wave fiber laser is rapidly modulated to investigate the possibilities to improve laser surface texturing processes by periodically changing the interaction between the surface tension in the melt pool and the vapor pressure created during high power laser processing. It was found that the intermittent nature of modulated continuous wave laser radiation can improve the melt expulsion from the processing area, leading to high material removal rates and ablation efficiencies while also limiting the heat input into the substrate material.
DOI: 10.2961/jlmn.2023.02.2009
Keywords: surface texturing, modulated cw-laser radiation, melt expulsion, drilling, fast modulation, ablation efficiency, µs pulses.

1. Introduction

Modern continuous-wave (cw) fiber lasers feature ever increasing output powers in compact form factors, excellent beam qualities, high stability and reliability and increased efficiencies. Another property, the ability to modulate the output power at high frequencies, has also improved significantly in recent years, but so far remained largely unnoticed or at least unused in most material processing applications. In this work we investigate the potential of laser surface treatment of metals using a single-mode cw-fiber laser, modulated at up to 100 kHz, allowing rise and fall times of less than 10 µs [1]. When compared to typically used short-pulsed laser systems, cw or quasi-cw beam-sources exhibit high average powers at moderate costs, making them an attractive alternative for large area-surface treatment [2] or drilling applications [3]. While short-pulsed and ultrafast laser systems are the first choice for applications requiring highest precision and repeatability, their limited average power, higher complexity, lower reliability and the higher cost of high average power ultrafast laser systems limit their applicability for many industrial tasks.

The laser-material interaction in structuring, drilling and ablation processes strongly depends on the applied pulse duration. The extremely high energy densities of ultrashort pulses in the femto- to picosecond regime lead to non-linear absorption effects as well as phase explosions, where a mixture of overheated liquid droplets and vapor expands rapidly from the interaction zone [4]. Moreover, the limited thermal diffusion depth leads to a decreased heat affected zone, since most of the heated material is removed from the interaction zone before the heat can be transferred to the surrounding material [5]. In contrast, longer pulse durations in the nanosecond regime lead to a predominantly thermal interaction, characterized by melting and evaporation as well as melt expulsion due to the recoil pressure [6]. Continuous wave lasers are rarely used for surface texturing and ablation processes, since the long interaction times would lead to significant heating of the substrate material and only small quantities of the material are removed, comparable to unwanted spatter in welding applications. To improve the material removal rate with cw lasers, a remote ablation cutting process can be applied [7]. In this process the laser beam is moved over the surface of the part very quickly. This greatly increases the dynamics of the interaction between the vapor phase and the melt, leading to improved melt expulsion out of the cutting kerf [8]. However, due to the nature of this process, this can only be applied to continuous kerfs, has limited ablation depths, and requires very high laser powers and high-speed deflection units. Therefore, this process is mostly used for cutting thin foils or generating straight grooves in thicker materials.

In this work we investigate the process of laser surface structuring using a single-mode continuous wave fiber laser at high modulation frequencies. The process is compared to a remote ablation cutting process to evaluate the influence of dynamically changing the equilibrium conditions between the vapor pressure and the recoil pressure in the melt pool by rapidly moving the beam and rapidly altering the applied laser power. The generated structures are compared in metallographic cross sections and the ablation efficiency is determined. The achieved efficiencies are then compared to a theoretical model and literature values from short- and ultrashort-pulsed laser ablation processes.

2. Materials and Methods

DC04 (1.0338) steel sheets with a thickness of 1 mm are used for the majority of the experiments. For comparison, an aluminum alloy EN-AW7075 (3.4365) is applied to investigate the influence of the higher reflectivity and different thermal properties on the laser-material interaction.

The optical setup applied in this work consists of a nlight CFL-700 single mode ($M^2 \leq 1.1$) ytterbium fiber laser with a maximum power of 700 W, a modulation frequency of up to 100 kHz and rise and fall times of approximately 2 µs. The laser beam is collimated to a beam diameter of 10.5 mm ($1/e^2$) and deflected using a Raylase SuperScan SC-30 galvanometer scanner. The beam is focused onto the workpiece by a F-Theta lens with a focal length of 163 mm (SillOptics S4LFT2163) resulting in a calculated focal diameter of 24 µm with gaussian intensity distribution. A total scan path of 1.2 m consisting of 40 parallel lines at a hatching distance of 375 µm is created on the samples.

The material removal rate is determined by weighing the samples before and after processing using an analytical scale. Metallographic cross sections are examined and photographed using reflective light microscopy (Carl Zeiss Axio Imager A2, Axiocam 305). In a preliminary study we examined suitable combinations of scanning speeds, pulse rates and average laser power [9]. The average laser power was kept constant at 500 W, resulting in a constant duty cycle of 71.4 % with the maximum available laser power of 700 W. To investigate the influence of the rise and fall times of the beam source, the integrated pulse shaping capability of the laser was used. Fig 1 shows the applied pulse shapes with a pulse frequency of 10 kHz and ramps of 2 µs, 10 µs and 30 µs at the beginning and end of the laser pulses.

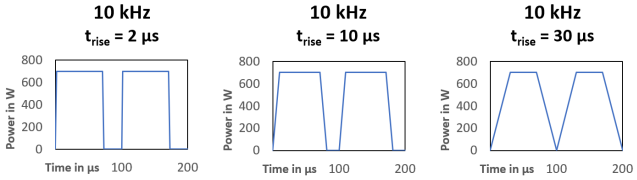

Fig. 1 Applied pulse shapes to investigate the influence of the rise and fall times of the modulated radiation at a pulse frequency of 10 kHz with an average power of 500 W.

The ablation efficiency was calculated using the measured mass loss of the samples and the applied laser parameters. The achieved ablation efficiencies were compared to literature values of other ablation processes using pulse lengths in the ns to fs regime and a basic theoretical model as applied in [4], which estimates the processing efficiency based on the applied laser energy per ablated volume, compared to the theoretically required energy to melt and evaporate this volume of material. The applied material parameters used for this calculation are summarized in Table 1. The influence of the composition of the alloys is neglected for this rough calculation, therefore the values of pure iron were applied instead of the DC04 steel. Additionally, the properties of aluminum are given for comparison.

Table 1 Thermal properties of iron and aluminum

Parameter	Iron	Aluminum	Unit
Melting Point	1812	933	K
Boiling Point	3134	2743	K
Density	7.874	2.699	g/cm³
Melting Enthalpy	247	397	J/g
Evaporation Enthalpy	6088	10525	J/g
Specific Heat Capacity	0.449	0.897	J/gK
Thermal Conductivity	80	235	W/mK

3. Results and Discussion

3.1 Geometry and microstructure

Compared to cw processing at high scanning speeds, the application of power modulation at frequencies between 10 and 30 kHz leads to much cleaner processing results with reduced melt adhesion and smaller heat affected zones. Fig 2 shows a comparison of the cross sections through the kerf created by continuous wave laser radiation as compared to laser radiation modulated at 20 kHz at a scanning speed of 4 m/s. In the cw process shown in Fig 2 a) there is a significant amount of resolidified melt and a large heat affected zone. The kerf created by modulated radiation has approximately the same dimensions as the heat affected zone in the cw process, but there is only minimal melt residue and a small heat affected zone, as shown in Fig. 2 b). This indicates that the melt is expulsed very efficiently in the pulsed process.

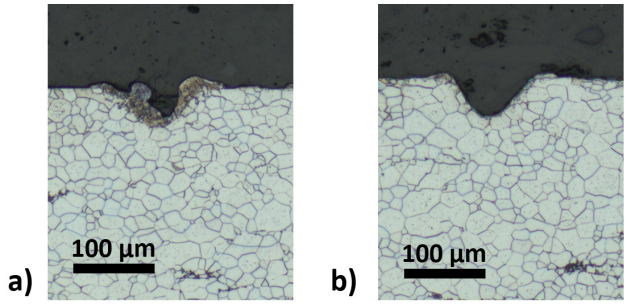

Fig. 2 Cross section through kerf created at scanning speed of 4 m/s and a cw power of 700 W (a) and modulated at 20 kHz with an average power of 500 W (b).

When applying multiple passes of the laser beam over the same geometry, this behavior remains mostly unchanged. Figure 3 shows the cross sections through the kerf created by continuous wave laser radiation as compared to modulated radiation with a pulse frequency of 10 kHz at a scanning speed of 4 m/s. In the cw process the kerf depth created by remote ablation cutting is significantly enlarged as compared to the single irradiation, but there is a large heat affected zone and melt adhesions forming a burr at the edges of the kerf, see Fig. 3 a) The structures created by modulated radiation have a slightly higher aspect ratio, and still show very small heat affected zones and minimal melt residue inside the cavity and smaller burrs at the edges as shown in Fig. 3 b). This indicates that the liquid melt can

be expelled even from deeper structures, limiting the heat transfer from the molten material to the substrate.

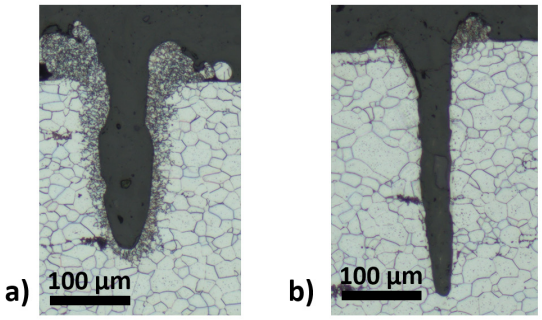

Fig. 3 Cross section through kerf created by 4 successive irradiations at scanning speed of 4 m/s and a cw power of 700 W (a) and modulated at 10 kHz with an average power of 500 W (b).

One of the advantages of the process is, that compared to remote ablation cutting the structuring depth can not only be achieved by multiple successive irradiations but can instead be controlled by the scanning speed and pulse duration. By applying slower scanning speeds and longer pulse durations a deeper keyhole is created, allowing the generation of higher structuring depths in a single irradiation as shown in Fig. 4 a, with a depth of 140 µm at a scanning speed of 1.2 m/s. By the repeated application of longer pulses at lower scanning speeds or stationary locations, very high aspect ratios can be generated. Fig 4 b) shows an example of an almost complete penetration through a 1 mm thick steel sheet after 4 irradiations with a pulse frequency of 10 kHz and a scanning speed of 1.2 m/s.

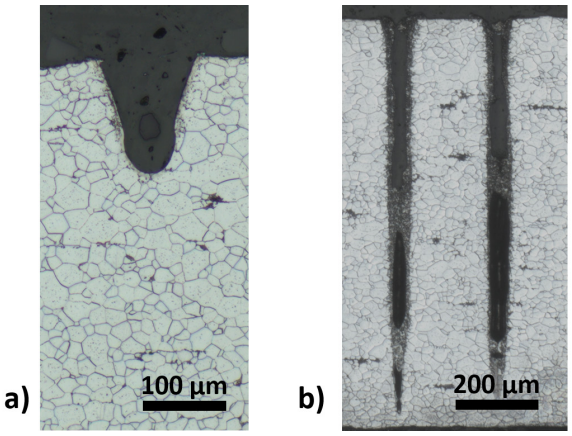

Fig. 4 Kerf created by single irradiation (a) and high aspect ratio holes created by 4 successive irradiations (b) with a pulse frequency of 10 kHz and a scanning speed of 1.2 m/s.

3.2 Ablation rate

The material removal rates of the modulated process were compared to continuous wave processing at two scanning speeds of 1.6 m/s with a single irradiation and at 4 m/s and 4 successive irradiations. At 1.6 m/s the material removal rates of the cw processes are very small, since the movement of the beam does not lead to sufficient melt pool dynamics to cause efficient melt expulsion from the kerf. By modulating the laser power at 10 kHz, the material removal rate is increased by a factor of 33 when compared to the cw process at 700 W and a factor of 49 when compared to the cw process at the same average power of 500 W as shown in Fig 5. The ablation rates achieved with rise and fall times of 2 µs and 10 µs are almost identical. In contrast, when the rise and fall times were programmed to 30 µs the material removal rate is reduced by approximately 30 %.

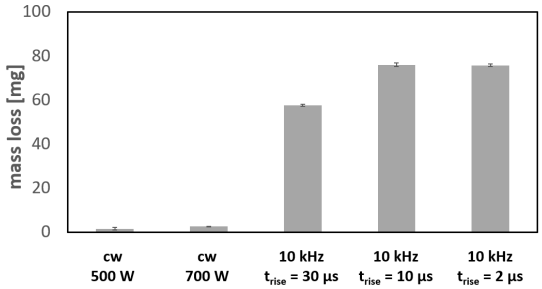

Fig. 5 Material removal rates of cw processes compared to modulated laser irradiation at 10 kHz with different rise and fall times at a scanning speed of 1.6 m/s.

At a scanning speed of 4 m/s the difference between the remote ablation cutting process with a cw power of 700 W and the modulated process becomes smaller, but the ablation rates are still higher as shown in Fig 6.

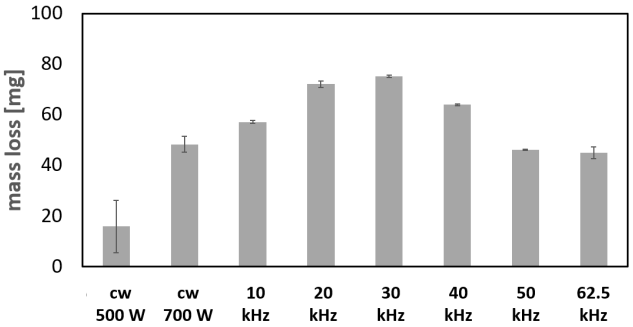

Fig. 6 Material removal rates of cw processes compared to modulated laser irradiation at 10 kHz with different rise and fall times at a scanning speed of 1.6 m/s.

Taking into consideration, that the applied average power is reduced to 500 W, this indicates a much more efficient melt expulsion and a lower heat load to the substrate. When comparing different modulation frequencies, a maximum in the ablation rate was found at 30 kHz. At the given duty cycle, this pulse frequency corresponds to a duration of approximately 10 µs between two successive pulses. This indicates, that there is a large drop in vapor pressure within this time span. Due to the disturbed equilibrium between the surface tension and the recoil pressure in the melt pool, the molten material is accelerated away from the processing zone, leading to efficient melt expulsion.

3.3 Ablation efficiency

The ablation efficiency was calculated for the 30 kHz parameter set shown in Fig. 6 using the measured mass loss and the density listed in Table 1. The calculated ablation efficiency is 0.95 mm³/minW at a pulse energy of 16.7 mJ and an ablated mass of 2.08 µg per pulse. These values are well above comparable ablation processes using µs, ns, ps, and fs pulses [4] and are very close to the theoretical values calculated for the evaporation of pure iron. The total applied energy during the structuring of the 1.2 m long scan path is 600 J. For comparison 69.8 J would be required to melt the ablated mass of 75 mg of iron, while 571 J would

be required for complete evaporation. Since thermal losses, the limited coupling efficiency of the infrared laser and other effects like for example the temperature dependence of some of the material properties are neglected in this model, these values confirm that indeed most of the material is removed in the liquid state and only a fraction of the material is evaporated. When looking at results in Fig. 5 this effect is even more pronounced since 76 mg are removed in a single irradiation at rise and fall times of 2 µs and 10 µs, leading to a comparable energy demand of 70.7 J for melting and 579 J for complete evaporation. However, during the 0.75 s of irradiation only 375 J are applied, leading to a calculated ablation efficiency of 1.54 mm³/minW at a pulse energy of 50 mJ and an ablated mass of 5.02 µg per pulse.

3.4 Resolidification of the ejected melt

When applying this process to aluminum, a different phenomenon was observed as shown in the scanning electron microscope images in Fig. 7. Melt was ejected from the individual craters created during processing; however, large amounts of the aluminum melt resolidified during the ejection process, forming needle-like structures at the edge of the holes as shown in Fig 7 a). In contrast, the DC04-steel sample shown in Fig. 7 b) shows only minimal spatter around the craters, but no larger amounts of solidified melt. Instead a single spherical droplet can be found at the surface. This particle likely solidified in the air and landed on the surface near a neighboring crater. The processing parameters applied in this example were a single irradiation at a scanning speed of 2.4 m/s, a pulse rate of 10 kHz with 700 W power and a duty cycle of 71.4 %.

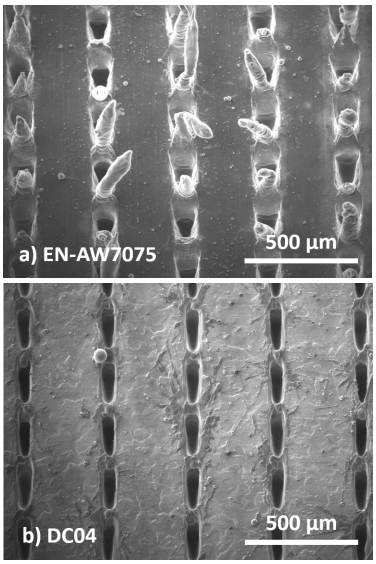

Fig. 7 Structured aluminum sample with partly resolidified melt, forming needle-like structures (a) compared to a steel sample processed with the same parameters (b).

The formation of these structures can be attributed to the thermal and optical properties of aluminum. Due to the higher reflectivity of aluminum compared to steel, less laser energy is absorbed by the material, leading to lower temperatures in the melt pool. Considering the larger temperature difference between the melting and boiling point, the relatively high heat capacity, evaporation enthalpy and boiling temperature of aluminum as shown in Table 1, much lower vapor pressures can be expected during the process. Therefore, the melt ejection velocities of aluminum from the melt pool after the end of a pulse are expected to be smaller. Due to the higher thermal conductivity the melt can cool down much quicker, enabling resolidification and the formation of these needle-like structures.

The structured surfaces showed hydrophobic to superhydrophobic properties, likely attributed to the combination of the surface topography and the formation of oxides on the needle-like structures.

4. Summary and Conclusion

The application of fast modulation of the laser power can significantly improve melt expulsion in laser structuring and ablation processes, leading to high ablation efficiencies when compared to the application of short-pulsed laser systems. It was found, that for the investigated steel material, a time of approximately 10 µs between two successive pulses and rise and fall times of 10 µs or less lead to the highest ablation rates.

The availability of high average powers at moderate system costs makes this process very attractive for applications that do not require the highest processing precision but need a high productivity to be industrially viable. Furthermore, this approach can be applied for drilling applications, since the effective melt expulsion is beneficial for the creation of high aspect ratio holes in moderately thick materials.

Acknowledgments and Appendixes

This work was funded by the German Federal Ministry of Economic Affairs and Energy (BMWi) within the Central Innovation Programme for SMEs (ZIM) based on a resolution passed by the German Parliament (Grant number ZF4410005FH9).

References

[1] D. A. V. Kliner, B. Victor, C. Rivera, G. Fanning, D. Balsley, R. L. Farrow, K. Kennedy, S. Hampton, R. Hawke, E. Soukup, M. Reynolds, A. Hodges, J. Emery, A. Brown, K. Almonte, M. Nelson, B. Foley, D. Dawson, D. M. Hemenway, W. Urbanek, M. DeVito, L. DeVito, L. Bao, J. Koponen, and K. Gross: Proc. SPIE 10513, (2018) 105130.

[2] H. Exner, L. Hartwig, R. Ebert, S. Klötzer, A. Streek, J. Schille, and U. Löschner: Proc. LPM, (2010) 1.

[3] S. Marimuthu, M. Antar,.J. Dunleavey, D. Chantzis, W. Darlington and P. Hayward: Opt. Laser Technol., 94, (2017) 119.

[4] K.-H. Leitz, B. Redlingshöfer, Y. Reg, A. Otto, and M. Schmidt: Phys. Proc., 12, (2011) 230.

[5] V. Villerius, H. Kooiker, J. Post and Y. T. Pei: Int. J. Mach. Tools Manuf., 138, (2019) 27.

[6] E. Williams and E. B. Brousseau: J. Mater. Process. Technol., 232, (2016) 34.

[7] P. Hellwig, K. Schricker and J. P. Bergmann: Proc. LiM, (2019) 24.

[8] M.F. Zaeh, J. Moesl, J. Musiol, and F. Oefele: Phys. Proc. 5 (A), (2010) 19.

[9] A. Schkutow and T. Frick: Procedia CIRP, 111, (2022) 732.

(Received: July 12, 2023, Accepted: September 13, 2023)